CHAPTER 5

ADSORPTION ISOTHERM AND KINETIC MODEL

After investigating the adsorption performance of all adsorbents (see Chapter 4). 10 adsorbents beads with high efficiency in adsorption cutting fluids were selected to study adsorption isotherm and kinetic. They include chitosan (CH, blended chitosan/PVA 1:1 (CH/PVA), benzoyl chitosan, quateraminated chitosan, chitosan-sodium lauryl sulfate (CH-SDS), chitosan-hexadecyltrimethy ammonium bromide (CH-C-Tab), chitosan- polyoxyethylene sorbitanmonooleate (CH-Tween 80), blended chitosan/PVA-sodium lauryl sulfate (BCH-SDS), blended chitosan/PVA-hexadecyltrimethy ammonium bromide (BCH-C-Tab) and blended chitosan/PVA-polyoxyethylene sorbitanmonooleate (BCH-Tween 80). The adsorption isotherm and kinetic of all adsorbents are presented in the following sections.

5.1. Adsorption isotherm

The adsorption isotherm model describes how adsorbate interacts with adsorbents and provides comprehensive understanding of the nature of interaction this is essential for the most effective use of the adsorbent. This is thus essential to correlate the equilibrium data by either theoretical or empirical models for designing a perfect operating adsorption system for industrial effluents. In the present investigation, the equilibrium data was analyzed according to the linear form of Langmuir, Freundlich and BET model of adsorption isotherm. The characteristics of each model are described as follow

The Langmuir isotherm assumes that intermolecular forces decrease rapidly with distance and this leads to the prediction that coverage of adsorbent by adsorbate is of a monolayer type. In other word, this isotherm assumes that a single adsorbate binds to a single site on the adsorbent and that all surface sites on the adsorbent have the same affinity for the adsorbate. Further, it is assumed that once a particular site of the adsorbent is occupied by an adsorbate molecule, no further adsorption takes place at that site. Theoretically, adsorbent has a finite number of sites and once all these sites are occupied by adsorbate further adsorption cannot take place. The Langmuir equation was originally developed to describe individual chemical adsorption and is applicable to physical adsorption (monolayer) within a low concentration range of adsorbate [43]. The Langmuir isotherm is expressed as

$$\frac{1}{q_e} = \frac{1}{q_0} + \frac{1}{K_L q_0}\frac{1}{C_e} \qquad (5.1)$$

where q_e is the amount of cutting fluids adsorbed per unit weight of adsorbents at equilibrium concentration (mg/g), C_e is the final concentration in the solution (mg/l), q_0 is the maximum adsorption at monolayer coverage (mg/g) and K_L is the adsorption equilibrium constant (l/mg).

In the case of Freundlich isotherm it describes the heterogeneous system and reversible adsorption. This is not restricted to the monolayer formation. This model predicts that adsorbate concentration in the adsorbent will increase with increase in adsorbate concentration in the solution. Freundlich equation is generally suitable for high concentration and middle concentration environmental and is not suitable for low concentration environmental because it does not meet the requirements of Herny's law [43]. The Freundlich isotherm is expressed as

$$q_e = K_f C_e^{1/n} \qquad (5.2)$$

where q_e is the amount of cutting fluid adsorbed per unit weight of adsorbents at equilibrium concentration (mg/g), C_e is the final concentration in the solution (mg/l), K_F is a Freundlich constant representing the adsorption capacity (mg/g)(l/mg)^n and n is a constant depicting the adsorption intensity (dimensionless).

The BET isotherm is an extension of the Langmuir isotherm to account for multilayer adsorption of adsorbate. This isotherm assumes that a number of layers of adsorbate accumulate at the surface and that the Langmuir isotherm applies to each layer. The BET isotherm is expressed as

$$\frac{C_e}{(C_s - C_e)x/m} = \frac{1}{K_B X_m} + \frac{K_B - 1}{K_B X_m}\left(\frac{C}{C_s}\right) \qquad (5.3)$$

where x is the amount of cutting fluids adsorbed (g), m is the weight of adsorbents (g), X_m is the amount of cutting fluids adsorbed in form a complete monolayer (mg/g), C_s is the saturation concentration of cutting fluids (mg/l), C_e is the concentration of cutting fluids in emulsion equilibrium (mg/l) and K_B is the BET constant.

In order to decide which type of isotherm better fit the experimental results, data were ploted $1/q_e$ versus $1/C_e$ for the Langmuir isotherm, log q_e versus log C_e for the Freundlich isotherm and $C_e/(Cs-C_e)(x/m)$ versus C_e/C_s for the BET isotherm. The suitable model for each adsorbent can be determined by calculation the relative coefficient (R^2) values. The example plots of experimental data presents in illustration Figure 5.1 to Figure 5.3, respectively. Table 5.1 shows the result of all adsorbents. It was found that blended chitosan/PVA 1:1, CH-C-Tab, CH-Tween 80, BCH-C-Tab and BCH-Tween 80 are adsorbents that fit well to the Langmuir isotherm. The relative coefficients of the experiments are 0.966, 0.978, 0.983, 0.973 and 0.998, respectively. The numerical values of the Langmuir isotherm constants were determined as q_0 equal

0.08, 7.14, 0.02, 0.003 and 0.001 mg/g, respectively. The q_0 of CH-C-Tab is the highest of those adsorbents.

Essential features of the Langmuir isotherm can also be expressed in terms of dimensionless equilibrium parameter R_L, which is equal to $1/(1 + K_L C_0)$ where K_L is the Langmuir constant as described above and C_0 is the initial cutting fluids concentration. Value of R_L less than one but greater than zero indicates favourable adsorption. R_L values calculated at different initial effluent concentrations are well within the defined range and this indicates favourable adsorption. The parameter shows the shapes of the isotherms according to Table 5.2 [40].

The results of separation factor of their adsorbents showed that blended chitosan/PVA 1:1, CH-C-Tab, CH-Tween 80, BCH-C-Tab and BCH-Tween 80 display a separation factor between 0 – 1. This value proves that the adsorbents adsorbe cutting fluids as the Langmuir isotherm. Thus the blended chitosan/PVA 1:1, CH-C-Tab, CH-Tween 80, BCH-C-Tab and BCH-Tween 80 display adsorption of cutting fluids as a monolayer adsorption processes.

For the case of chitosan, the plot of log q_e versus log C_e is based on Equation 5.2. The experimental results are shown in Figure 5.2, it can be see that chitosan adsorbs cutting fluids and fits very well with the Freundlich isotherm. This result is shown in Table 5.1. The values of K_F and n are 0.07 and 0.58, respectively. A value of n larger than one suggests that the amount of adsorption will approach a limit [44]. In-addition 1/n of the Freundlich isotherm is a measure for the adsorption intensity. Therefore, the value on "n" can be divided into three cases i.e., n = 1 indicate that the partition between the two phases is independence of the concentration, 1/n below one indicates a normal Langmuir isotherm and finally 1/n above one is indicative for a cooperative adsorption [45]. Hence from this study, it can be see that value of n is lower than one

thus the amount of adsorption is farther to a limit. Thus the chitosan may display adsorption cutting fluids ether a heterogeneous adsorption according to n value.

For the case of benzoyl chitosan, quateraminated chitosan, CH-SDS and BCH-SDS, it can be see that they adsorb cutting fluids and fit very well with the BET isotherm, as show in Table 5.1.

The BET constant "a" describes the energy interaction between solute and adsorbent surface [12]. The constant K_B of quateraminated chitosan was the highest at 585.9 followed by benzoyl chitosan at 24.52. The constant K_B of both CH-SDS and BCH-SDS were equivalent at 1.00. Therefore cutting fluids were adsorbed on benzoyl chitosan, quateraminated chitosan, CH-SDS and BCH-SDS as a more complicated multi-layer.

The mechanism of adsorption may involve four steps: (1) diffusion of cutting fluids to the boundary surface of adsorbent; (2) diffusion of liquid film at the pores of adsorbent; (3) diffusion into the pores of adsorbent; (4) adsorption of cutting fluids on the internal surface of the adsorbent.

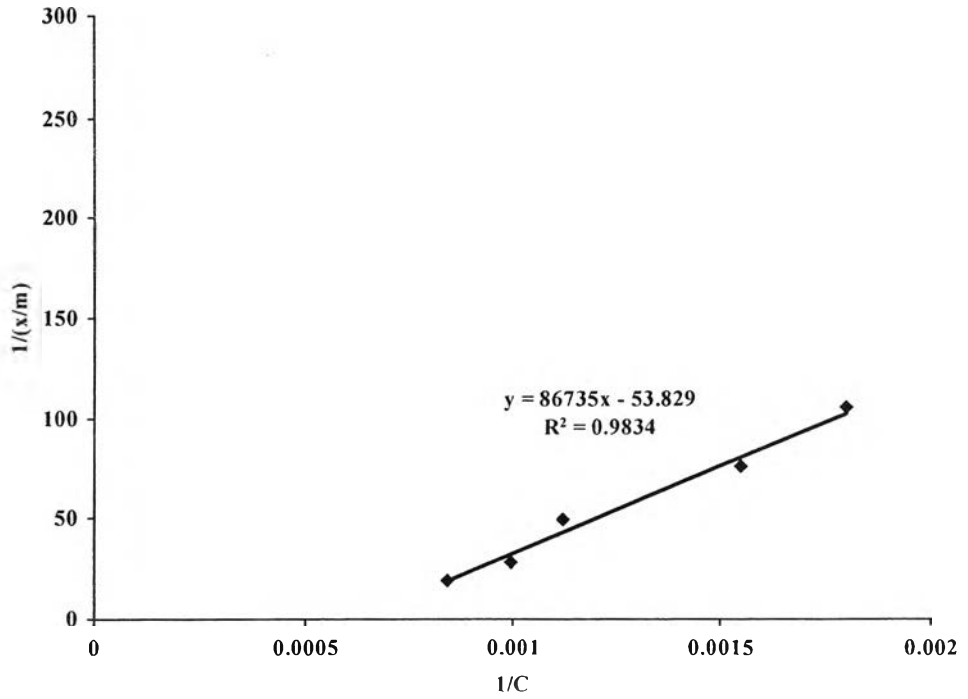

Figure 5.1 Langmuir isotherm of cutting fluids on CH-Tween 80

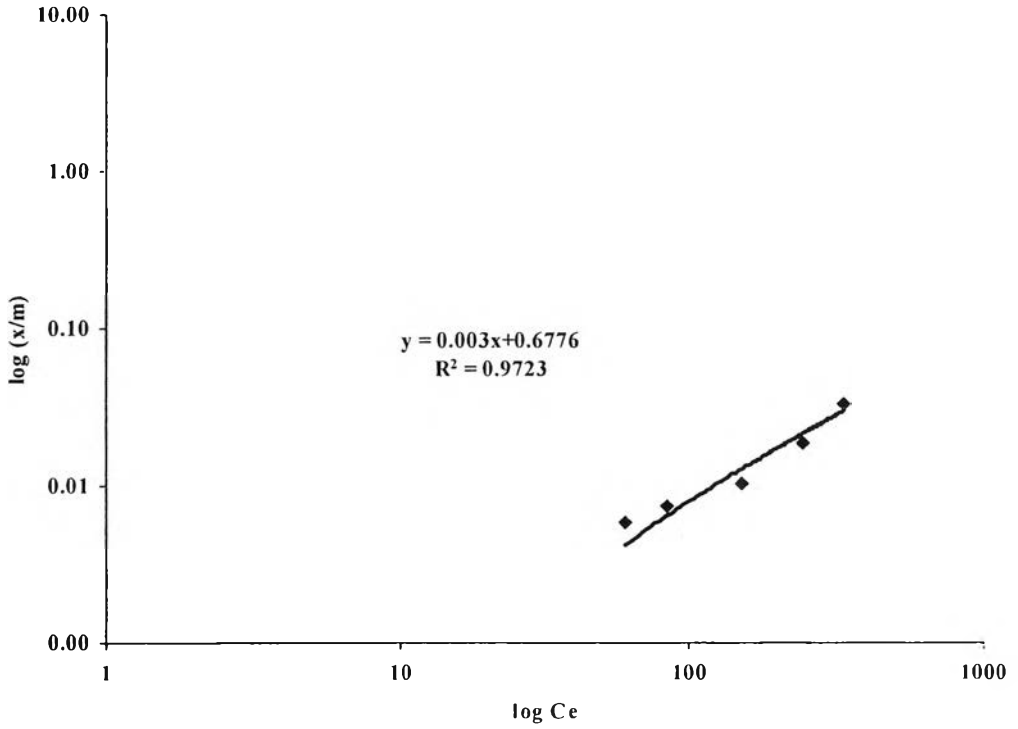

Figure 5.2 Freundlich isotherm of cutting fluids on chitisan

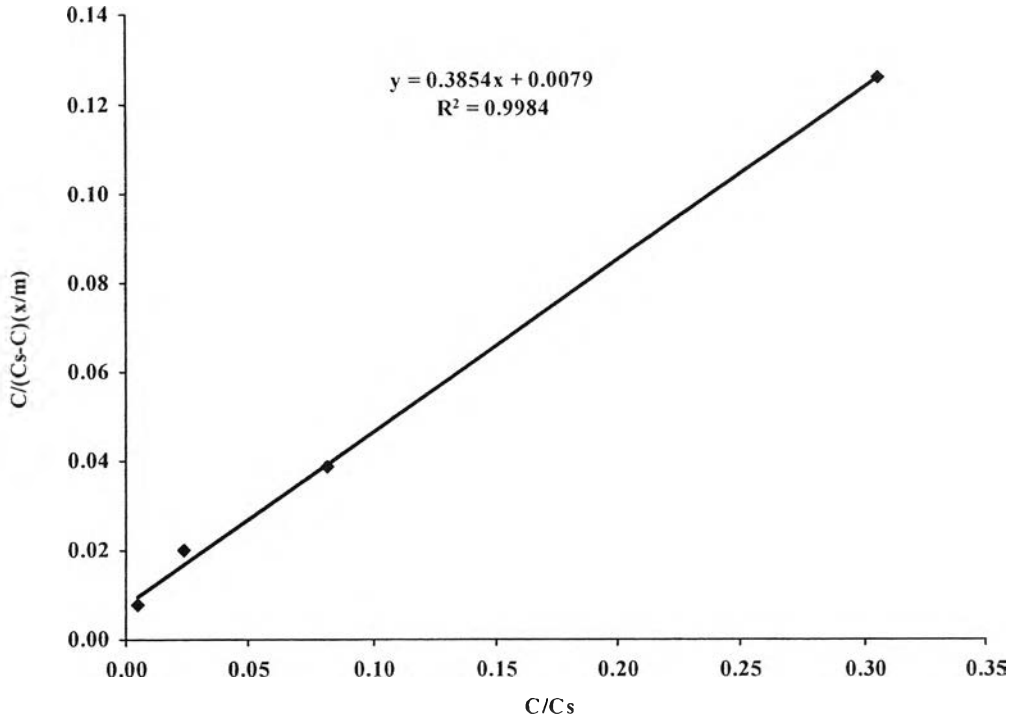

Figure 5.3 BET isotherm of cutting fluidson BCH-SDS

Table 5.1 Adsorption isotherms for adsorption cutting fluids onto adsorbents

Adsorbents	Langmuir				Freundlich			BET		
	K_L	q_0	R_L	R^2	K_F	n	R^2	K_B	X_m	R^2
Chitosan	0.0050	0.30	0.002	0.927	0.07	0.58	**0.972**	1.16	12.78	0.806
Blended chitosan/PVA 1:1	0.0010	0.08	$1.3x10^{-2}$	**0.966**	0.02	0.44	0.951	197	0.00	0.452
Benzoyl chitosan	0.0001	0.31	0.001	0.742	0.01	0.49	0.833	24.52	0.03	**0.865**
Quateraminated chitosan	0.0170	0.02	0.003	0.927	0.01	0.49	0.697	585.90	0.01	**0.979**
CH-SDS	0.0270	1.34	$1.5x10^{-5}$	0.804	0.86	180.56	0.637	1.00	47.30	**0.986**
CH-C-Tab	$1.2x10^{-5}$	7.14	$4.1x10^{-6}$	**0.978**	0.58	0.93	0.876	-4.22	0.31	0.957
CH-Tween 80	0.0010	0.02	$3.1x10^{-2}$	**0.983**	-0.03	-	0.920	848.87	0.00	0.612
BCH-SDS	0.0013	2.58	$7.7x10^{-6}$	0.953	1.02	122.82	0.884	1.00	126.20	**0.998**
BCH-C-Tab	-	0.003	$8.3x10^{-3}$	**0.973**	-10.3	-	0.905	$-8.6x10^{5}$	0.00	0.842
BCH-Tween 80	-	0.001	$2.4x10^{-2}$	**0.998**	-3.89	-	0.509	$-3.6x10^{5}$	0.00	0.700

Table 5.2 Effect of the separation factor on isotherm shapes

R_L Value	Type of isotherm
$R_L > 1$	Unfavorable
$R_L = 1$	Linear
$0 < R_L < 1$	Favorable
$R_L = 0$	Irriversible

5.2. Pseudo-first-order and pseudo-second-order models

Two kinetic model i.e. pseudo-first-order and pseudo-second-order, were used to test experimental data and analyze the kinetics of the adsorption process [46-48]. The kinetic models were developed to find intrinsic kinetic adsorption constants. Azizian, S., [49] determined the conditions for using pseudo first order and pseudo second order models and also identified the real meaning of their observed rate coefficients. Consider in the adsorption and desorption of solute A in solution

$$A + * \underset{k_d}{\overset{k_a}{\longleftrightarrow}} A_{(a)} \qquad (5.4)$$

where k_a and k_d are the adsorption and desorption rate constants and * represents the vacant site. The adsorption, v_a and desorption rates, v_d can be calculated from Equation 5.5 and 5.6.

$$v_a = k_a C_t (1 - \theta) \qquad (5.5)$$

$$v_d = k_d \theta \qquad (5.6)$$

where θ is the coverage fraction ($0 \leq \theta \leq 1$) and C_t is the molar concentration of solute at any time. The overall rate equation is

$$\frac{d\theta}{dt} = v_a - v_d \qquad (5.7)$$

$$\frac{d\theta}{dt} = k_d C_t (1 - \theta) - k_d \theta \qquad (5.8)$$

By adsorption of solute from solution onto the surface of adsorbent, the concentration of solute in solution decreases as follow;

$$C_t = C_0 - \beta\theta \qquad (5.9)$$

where C_0 is the initial molar concentration of solute, C_t is its molar concentration at any time, θ is surface coverage fraction, and β is

$$\beta = \frac{m_c q_m}{M_w V} \qquad (5.10)$$

where m_c is the mass (g) of sorbent, q_m is the maximum capacity of sorbent, M_w is the molar weight of solute (g/mol), and V is the volume of solution (l). One can rewrite β as

$$\beta = \frac{C_0 - C_e}{\theta_e} \qquad (5.11)$$

where C_e is the equilibrium molar concentration of solute and θ_e is the equilibrium coverage fraction. By inserting Equation 5.9 into Equation 5.8

$$\frac{d\theta}{dt} = k_a(C_0 - \beta\theta)(1-\theta) - k_d\theta \qquad (5.12)$$

Equation 5.12 was the general equation which was used at different conditions for derivation of various kinetic models of adsorption.

5.2.1. Derivation of pseudo-first-order model

If the experimental condition be such that the initial concentration of solute, C_0 is very high compared to βθ ($C_0 >> \beta\theta$), then one can ignore the βθ term in Equation 5.12, and therefore

$$\frac{d\theta}{dt} = k_a C_0(1-\theta) - k_d\theta \qquad (5.13)$$

$$\frac{d\theta}{dt} = k_a C_0 - (k_a C_0 + k_d)\theta \qquad (5.14)$$

By definition of

$$f = k_a C_0 \tag{5.15}$$

$$k_1 = k_a C_0 + k_d \tag{5.16}$$

and substitution of Equation 5.15 and Equation 5.16 into Equation 5.14, to obtain

$$\frac{d\theta}{dt} = f - k_1\theta \tag{5.17}$$

Integration of Equation 5.17 gives

$$\int_0^{\theta} \frac{d\theta}{f - k_1\theta} = \int_0^{t} dt \tag{5.18}$$

$$\ln(1 - \frac{k_1}{f}\theta) = -k_1 t \tag{5.19}$$

Deriving Equation 5.16 with Equation 5.15 to obtain

$$\frac{k_1}{f} = \frac{k_a C_0 + k_d}{k_a C_0} \tag{5.20}$$

By defining the Equation constant as K = k_a/k_d and rewriting Equation 5.20,

$$\frac{k_1}{f} = \frac{KC_0 + 1}{KC_0} \tag{5.21}$$

At equilibrium dθ/dt = 0, Equation 5.14 at equilibrium converts to

$$\frac{1}{\theta_e} = \frac{KC_e + 1}{KC_e} \cong \frac{K_f}{f} \tag{5.22}$$

By inserting Equation 5.22 into Equation 5.19, to obtain

$$\ln\left(1 - \frac{\theta}{\theta_e}\right) = -k_1 t \tag{5.23}$$

It is known that

$$\frac{\theta}{\theta_e} = \frac{q}{q_e} \tag{5.24}$$

Therefore, Equation 5.23 converts to

$$\ln\frac{(q_e - q_t)}{q_e} = -k_1 t \tag{5.25}$$

or

$$\log(q_e - q_t) = \log q_e - \frac{k_1}{2.303} t \tag{5.26}$$

where k_1 is the rate constant of the pseudo-first-order model.

The values of k_1 and q_e are determined from the slope and intercept of the plots of log ($q_e - q_t$) versus t, respectively.

5.2.2. Derivation of pseudo-second-order model

If the initial concentration of solute, C_0 is not too high for the βθ term in Equation 5.12 to be ignored, then for derivation of the rate law, one can integrate Equation 5.12 directly. By rearrangement of Equation 5.12 to obtain

$$\frac{d\theta}{dt} = k_a\beta\theta^2 - \left(\beta + C_0 + \frac{1}{K}\right)k_a\theta + k_aC_0 \qquad (5.27)$$

or

$$\frac{d\theta}{dt} = a\theta^2 + b\theta + f \qquad (5.28)$$

where

$$a = k_a\beta \qquad (5.29)$$

$$b = -\left(\beta + C_0 + \frac{1}{K}\right)k_a \qquad (5.30)$$

$$f = k_aC_0 \qquad (5.31)$$

By integrating of Equation 5.28

$$\int_0^{\theta} \frac{d\theta}{a\theta^2 + b\theta + f} = \int_0^{t} dt \qquad (5.32)$$

$$\frac{1}{\sqrt{b^2 - 4af}}\left[\ln\frac{2a\theta + b - \sqrt{b^2 - 4af}}{2a\theta + b + \sqrt{b^2 - 4af}} - \ln\frac{b - \sqrt{b^2 - 4af}}{b + \sqrt{b^2 - 4af}}\right] = t \qquad (5.33)$$

By definition of

$$\lambda = \sqrt{b^2 - 4af} \qquad (5.34)$$

$$\gamma = b - \lambda \qquad (5.35)$$

$$\xi = b + \lambda \qquad (5.36)$$

$$\ln\frac{\gamma}{\xi} = \tau \tag{5.37}$$

and substitution of the above equation into Equation 5.33 to obtain

$$\ln\left(\frac{2a\theta+\gamma}{2a\theta+\xi}\right) - \tau = \lambda t \tag{5.38}$$

therefore

$$\theta = \frac{\xi e^{\lambda t+\tau} - \gamma}{2a(1-e^{\lambda t+\tau})} \tag{5.39}$$

Equation 5.39, represents the variation of surface coverage fraction (θ) with time. For justification of this equation, the boundary conditions $t = 0$ and $t = \infty$ are applied to Equation 5.39.

At t $\rightarrow$ 0 Equation 5.39 converts to

$$\theta_0 = \frac{\xi e^{\tau} - \gamma}{2a(1-e^{\tau})} \tag{5.40}$$

where the numerator Equation 5.40 is zero, so that $\theta_0 = 0$ at $t = 0$

At t $\rightarrow \infty$ (or equilibrium), Equation 5.39 becomes

$$\theta_e = -\frac{\xi}{2a} \tag{5.41}$$

or

$$\theta_e = \frac{KC_e}{1+KC_e} \tag{5.42}$$

which is the Langmuir adsorption isotherm. Equation 5. 39 can be rearranged to equation

$$\theta = \frac{\xi e^{\lambda t} e^{\tau} - \gamma}{2a(1-e^{\lambda t} e^{\tau})} \tag{5.43}$$

and by using Equation 5.37

$$\theta = \frac{\xi\gamma(e^{\lambda t}-1)}{2a(\xi-\gamma e^{\lambda t})} \tag{5.44}$$

Small values of x have the following mathematical approximation

$$e^{x} \approx 1 + x \tag{5.45}$$

So by replacement of $x = \lambda t$ and using the above approximation to Equation 5.44, to obtain

$$\theta \approx \frac{\xi\gamma(1+\lambda t-1)}{2a(\xi-\gamma-\gamma\lambda t)} \tag{5.46}$$

or

$$\theta \approx \frac{\xi\gamma\lambda t}{2a(2\lambda-\gamma\lambda t)} \tag{5.47}$$

It is known that at $t = 0$, the initial coverage fraction was zero ($\theta_0 = 0$), which was compatible with the above equation. By substitution of Equation 5.41 into Equation 5.47

$$\theta \approx \frac{-\theta_e\gamma\lambda t}{(2\lambda-2\gamma\lambda t)} \tag{5.48}$$

Rearrangement of Equation 5.48 yields

$$\frac{1}{\theta} = \frac{2}{\gamma\theta_e}\frac{1}{t} + \frac{1}{\theta_e} \tag{5.49}$$

or

$$\frac{t}{\theta} = -\frac{2}{\gamma\theta_e} + \frac{1}{\theta_e}t \tag{5.50}$$

By replacement of $\theta = q/q_m$ and $\theta_e = q_e/q_m$, to obtain

$$\frac{t}{q} = -\frac{2}{\gamma q_e} + \frac{1}{q_e}t \tag{5.51}$$

By definition of k_2 as

$$k_2 = -\frac{\gamma}{2q_e} \tag{5.52}$$

and substitution of Equation 5.52 into Equation 5.51

$$\frac{t}{q} = \frac{1}{k_2 q_e^2} + \frac{1}{q_e}t \tag{5.53}$$

or

$$\frac{t}{q_t} = \frac{1}{k_2 q_e^2} + \frac{1}{q_e}t \tag{5.54}$$

where k_2 is the rate constant of pseudo-second-order adsorption (mg/g-min).

From Equation 5.54

It is obvious that, Equation (5.54) k_2 and q_e can be calculated from the intercept and slope of straight-line plot of (t/q_t) versus t and there is no need to know any prior parameters. The suitable of kinetic models is tested by obtaining the correlation coefficient (R^2). Two kinetic models for adsorption from liquid adsorption, i.e, pseudo-first-order and pseudo-second-order, were derived and used in the many literatures [50-56]

Two kinetic models basically include all steps of adsorption such as external film diffusion, adsorption and internal particle diffusion. So they are pseudo model [43, 57]. In the present study, linear form of pseudo-first-order and pseudo-second-order kinetic rate models, were studied with the kinetic experimental data to examine the controlling mechanism of adsorption cutting fluids of all adsorbents. The parameters in the two models were determined from the linear plots of $\log(q_e-q_t)$ versus t for pseudo-first-order and t/q_t versus t for pseudo-second-order. Figure 5.4 and Figure 5.5 presents pseudo-first-order and pseudo-second-order of all adsorbents including chitosan, blended chitosan/PVA 1:1, benzoyl chitosan, quateraminated chitosan, CH-SDS, CH-C-Tab, CH-Tween 80, BCH-SDS, BCH-C-Tab and BCH-Tween 80. The validity of each model was checked by correlation coefficient. Table 5.3 to 5.6 shows the parameters of both kinetic models. It can be seen that the adsorption kinetic of cutting fluids follows the pseudo-second-order model. Correlation coefficients vary in the range 0.836 - 0.999 for pseudo-second-order, while pseudo-first-order model presents correlation coefficients varying in the range 0.001 – 0.967. This suggests that the adsorption of cutting fluids onto all adsorbents is not a pseudo-first-order. From the pseudo-second-order equation, a two-step linear relationship is obtained. The first-step is very much shorter than the second-step, see Figure 5.5. Since the pseudo-second-order equation is based on the adsorption capacity. It predicts the behavior

over the "whole" range of studies strongly supporting the validity and agrees with chemisorption or chemical reaction as rate-controlling mechanism [46, 48, 51]. The chemisorption or chemical sorption involve valency forces through sharing or exchange of electrons between adsorbent and adsorbate [47]. The straight linear line in plot t/q_t versus t proves a good agreement of experimental data with the pseudo-second-order kinetic model. Table 5.3 to 5.6 summarizes the computed results obtained for the pseudo-first-order and pseudo-second-order. The correlation coefficient for the pseudo-second-order kinetic model is almost equal to 1.0 for all adsorbents. Furthermore, the calculated q_e values in Table 5.3 – 5.6 obtained from the pseudo-second-order kinetic model agree very well with the q_e of the experimental data. On the contrary, the pseudo-first-order kinetic model does not give reasonable values. The calculated values are higher than the actual experimental values.

The k_1 and k_2 for both kinetic models indicated that adsorption rate of adsorbent. It was found that the rate constant k_2 of chitosan, blended chitosan/PVA 1:1 and CH-C-Tab, cutting fluids concentration 1.00 % w/v and pH 3, was higher than k_1. The rate constant k_1 of benzoyl chitosan, quateraminated chitosan, CH-SDS, CH-Tween 80, BCH-SDS, BCH-C-Tab and BCH-Tween 80, cutting fluids concentration 1.00 % w/v and pH 3, was higher than k_2. The rate constant k_2 of all adsorbents shows a rank from low to high of BCH-SDS, CH-SDS, CH-Tween 80, benzoyl chitosan, quateraminated chitosan, chitosan, CH-C-Tab and blended chitosan/PVA 1:1 were 0.0001, 0.0002, 0.0005, 0.0007, 0.0013, 0.0015, 0.0049 and 0.0068, respectively. From the rate constant, k_2 proves that the rate of cutting fluids adsorption by blended chitosan/PVA 1:1 was about 68, 49, 15, 8, 7, 5, and 2 times of CH-C-Tab, chitosan, quateraminated chitosan, benzoyl chitosan, CH-Tween 80, CH-SDS and BCH-SDS, respectively.

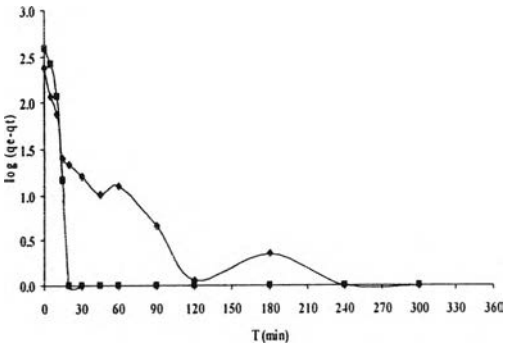

(a) ♦ chitosan, ■ blended chitosan /PVA 1:1

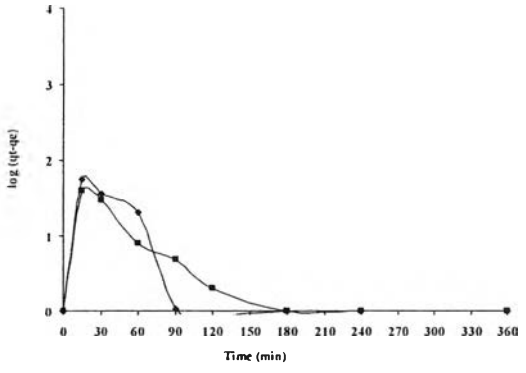

(b) ♦ benzoyl chitosan and ■ quateraminated chitosan

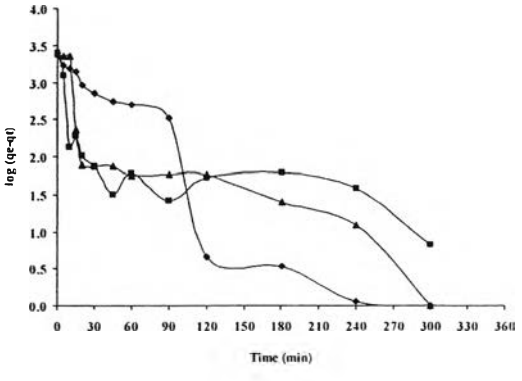

(c) ♦ CH-SDS, ■ CH-C-Tab and ▲ CH-Tween 80

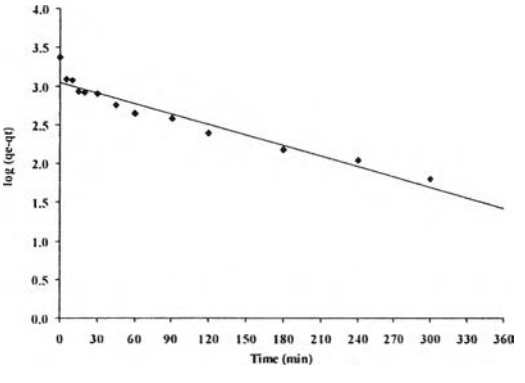

(b) ♦ BCH-SDS

Figure 5.4 Pseudo-first-order kinetic model for adsorption of cutting fluids onto various adsorbents

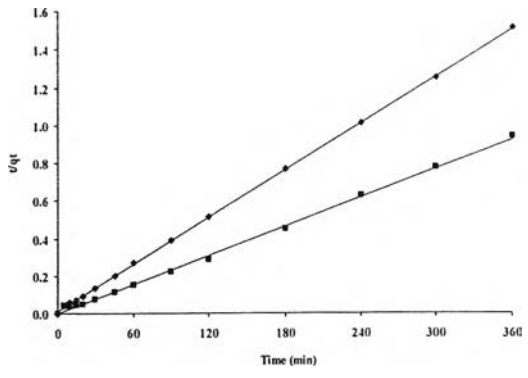

(a) ♦ chitosan and

■ blended chitosan /PVA 1:1

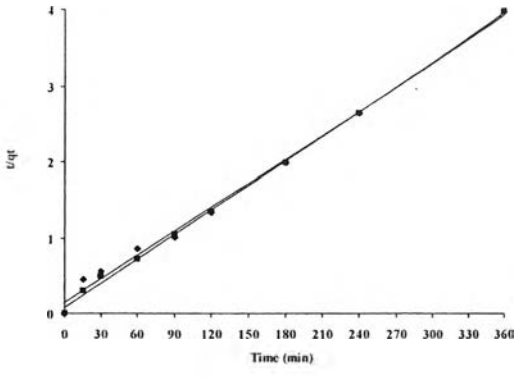

(b) ♦ benzoyl chitosan and

■ quateraminated chitosan

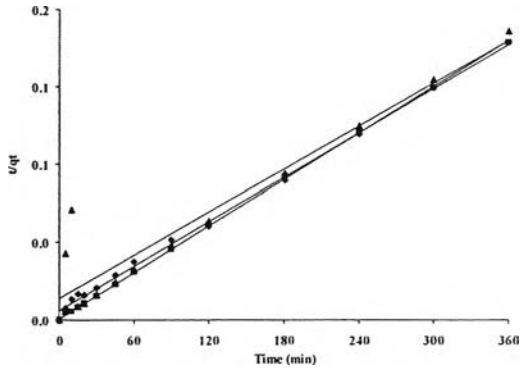

(c) ♦ CH-SDS, ■ CH-C-Tab

and ▲ CH-Tween 80

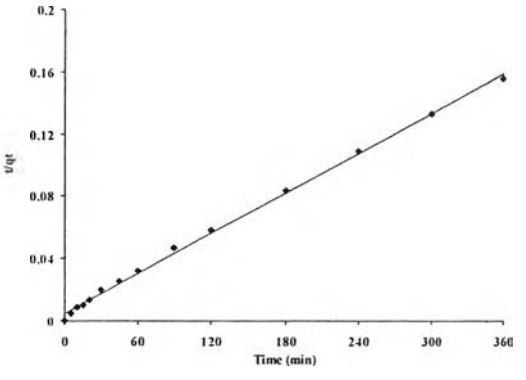

(b) ♦ BCH-SDS

Figure 5.5 Pseudo-second-order kinetic model for adsorption of cutting fluids onto various adsorbents

Table 5.3 Comparison of pseudo-first and-second orders calculated and experimental q_e and adsorption rate constants of chitosan and blended chitosan/PVA 1:1

Adsorbents	Concentration (w/v)	pH	Pseudo-first-order				Pseudo-second-order			
			q_e(mg/g) (cal)	q_e(mg/g) (exp)	k_1 (min^{-1})	R^2	q_e (mg/g) (cal)	q_e(mg/g) (exp)	k_2 (mg/g-min)	R^2
CH	0.10	3	-0.2441	20.27	0.0028	0.430	20.41	20.27	0.0421	0.999
	0.50	3	0.0128	185.81	0.0052	0.399	188.68	185.81	0.0094	0.999
	1.00	3	0.1038	237.61	0.0070	0.739	238.10	237.61	0.0015	0.999
	3.00	3	0.1139	130.63	0.0053	0.389	133.33	130.63	0.0094	0.995
	1.00	5	-0.8633	9.29	0.0007	0.070	10.73	9.29	0.0120	0.959
	1.00	7	-1.6383	8.45	0.0002	0.005	8.06	8.45	0.0352	0.993
	1.00	9	-0.4711	10.98	0.0015	0.198	10.76	10.98	0.0113	0.992
	1.00	11	-1.0969	10.56	0.0003	0.007	10.20	10.56	0.1404	0.996
CH/PVA	0.10	3	-0.1618	43.92	0.0034	0.381	45.45	43.92	0.0538	0.998
	0.50	3	0.0584	194.82	0.0037	0.333	196.08	194.82	0.0043	0.999
	1.00	3	0.0523	382.88	0.0058	0.291	384.62	382.88	0.0068	0.998
	3.00	3	0.1028	242.12	0.0060	0.543	243.90	242.12	0.0056	0.999
	1.00	5	-0.6142	11.68	0.0025	0.190	12.48	11.68	0.0131	0.993
	1.00	7	-0.6158	9.15	0.0021	0.240	8.98	9.15	0.2212	0.994
	1.00	9	-0.6633	11.26	0.0015	0.153	11.03	11.26	0.0162	0.997
	1.00	11	-0.8861	8.31	0.0007	0.070	8.37	8.31	0.0288	0.999

Table 5.4 Comparison of pseudo-first and-second-orders calculated and experimental q_e and adsorption rate constants of benzoyl chitosan and quateraminated chitosan

Adsorbents	Concentration (w/v)	pH	Pseudo-first-order				Pseudo-second-order			
			q_e (mg/g) (cal)	q_e (mg/g) (exp)	k_1 (min^{-1})	R^2	q_e (mg/g) (cal)	q_e (mg/g) (exp)	k_2 (mg/g-min)	R^2
BCH	0.20	3	-0.1631	16.27	0.0029	0.490	16.95	16.27	0.0057	0.994
	1.00	3	0.1548	90.78	0.0057	0.592	95.24	90.78	0.0007	0.994
	2.00	3	0.3571	172.24	0.0770	0.824	212.77	172.24	0.0001	0.892
	3.00	3	0.3304	114.49	0.0047	0.827	117.65	114.49	0.0001	0.912
	1.00	5	-2.0655	13.70	0.0006	0.139	12.12	13.70	0.0457	0.934
	1.00	7	0.0262	40.92	0.0017	0.148	39.37	40.92	0.0004	0.956
	1.00	9	-0.0789	24.96	0.0025	0.356	26.11	24.96	0.0022	0.969
	1.00	11	-0.0476	28.53	0.0021	0.305	29.24	28.53	0.0011	0.976
QCH	0.20	3	-0.1874	16.27	0.0028	0.394	16.16	16.27	0.0401	0.998
	1.00	3	0.1569	90.78	0.0055	0.737	93.46	90.78	0.0013	0.999
	2.00	3	0.3302	172.24	0.0067	0.927	181.82	172.24	0.0002	0.990
	3.00	3	0.2019	64.38	0.0055	0.880	67.57	64.38	0.0005	0.980
	1.00	5	-0.8996	19.52	0.0070	0.137	23.36	19.52	0.0151	0.999
	1.00	7	-0.1463	37.54	0.0022	0.383	37.74	37.54	0.0029	0.996
	1.00	9	0.0322	44.87	0.0028	0.332	46.95	44.87	0.0007	0.958
	1.00	11	-0.1506	19.89	0.0004	0.014	20.45	19.89	0.0022	0.882

Table 5.5 Comparison of pseudo-first and-second-orders calculated and experimental q_e and adsorption rate constants of CH-SDS, CH-C-Tab and CH-Tween 80

Adsorbents	Concentration (w/v)	pH	Pseudo-first-order				Pseudo-second-order			
			q_e(mg/g) (cal)	q_e (mg/g) (exp)	k_1 (min^{-1})	R^2	q_e (mg/g) (cal)	q_e (mg/g) (exp)	k_2 (mg/g-min)	R^2
CH-SDS	0.10	3	-0.5426	4.50	0.0013	0.232	4.37	4.50	0.3067	0.836
	0.50	3	0.2222	406.53	0.0081	0.534	416.67	406.53	0.0003	0.993
	1.00	3	0.3345	838.96	0.0100	0.677	833.33	838.96	0.0002	0.996
	2.00	3	0.4518	1725.23	0.0128	0.741	2000.00	1725.23	0.00003	0.993
	3.00	3	0.5120	2511.26	0.0128	0.906	2500.00	2511.26	0.00003	0.998
	5.00	3	0.5204	2173.42	0.0039	0.967	2500.00	2173.42	0.00001	0.958
	10.00	3	0.4487	796.17	0.0026	0.948	769.23	796.17	0.00003	0.951
	3.00	5	0.3998	849.10	0.0035	0.806	833.33	849.10	0.0001	0.997
	3.00	7	0.3316	747.75	0.0053	0.804	769.23	747.75	0.0005	0.999
	3.00	9	-0.4473	359.23	0.0019	0.070	357.14	359.23	0.0013	0.995
	3.00	11	-0.2480	309.68	0.0029	0.146	312.50	309.68	0.0035	0.999
CH-C-Tab	0.10	3	0.0849	25.90	0.0031	0.688	25.97	25.90	0.0014	0.939
	0.50	3	0.0473	207.21	0.0018	0.043	200.00	207.21	0.0006	0.981
	1.00	3	-0.0867	358.11	0.0022	0.056	357.14	358.11	0.0049	0.999
	2.00	3	0.4246	1638.51	0.0048	0.842	1666.67	1638.51	0.0001	0.999
	3.00	3	0.3740	2564.64	0.0047	0.481	2500.00	2564.64	0.0003	0.999
	3.00	5	0.2410	106.98	0.0060	0.714	109.89	106.98	0.0005	0.992
	3.00	7	0.0849	93.47	0.0059	0.494	94.34	93.47	0.0019	0.995
	3.00	9	-0.2306	42.79	0.0025	0.174	43.10	42.79	0.0220	0.995
	3.00	11	-0.3757	97.97	0.0020	0.001	96.15	97.97	0.0373	0.997
CH-Tween 80	0.10	3	-0.7055	24.77	0.0001	0.070	28.17	24.77	0.0030	0.962
	0.50	3	0.0678	189.19	0.0052	0.843	192.31	189.19	0.0004	0.993
	1.00	3	0.3318	716.22	0.0064	0.687	714.29	716.22	0.0005	0.999
	2.00	3	0.4229	1420.05	0.0064	0.723	1428.57	1420.05	0.0002	0.999
	3.00	3	0.4358	2422.30	0.0085	0.728	2500.00	2422.30	0.00003	0.912
	3.00	5	-0.3883	23.65	0.0021	0.123	28.25	23.65	0.0017	0.912
	3.00	7	0.1632	188.06	0.0049	0.515	188.68	188.06	0.0023	0.997
	3.00	9	0.2114	213.96	0.0038	0.567	212.77	213.96	0.0013	0.999
	3.00	11	-0.5272	141.89	0.0017	0.071	140.85	141.89	0.0017	0.998

Table 5.6 Comparison of pseudo-first and-second-orders calculated and experimental q_e and adsorption rate constants of BCH-SDS, BCH-C-Tab and BCH-Tween 80

Adsorbents	Concentration (w/v)	pH	Pseudo-first-order				Pseudo-second-order			
			q_e (mg/g) (cal)	q_e (mg/g) (exp)	k_1 (min^{-1})	R^2	q_e (mg/g) (cal)	q_e (mg/g) (exp)	k_2 (mg/g-min)	R^2
BCH-SDS	0.10	3	0.0860	38.29	0.0044	0.566	42.55	38.29	0.0004	0.804
	0.50	3	0.4244	413.29	0.0082	0.747	416.67	413.29	0.0009	0.999
	1.00	3	0.4244	846.85	0.0069	0.969	833.33	846.85	0.0001	0.999
	2.00	3	0.4631	1472.97	0.0045	0.920	1428.57	1472.97	0.00003	0.995
	3.00	3	0.4846	2310.81	0.0045	0.930	2500.00	2310.81	0.00003	0.998
	5.00	3	0.4428	819.82	0.0031	0.920	833.33	819.82	0.00005	0.972
	10.00	3	-0.6162	213.96	0.0017	0.745	238.10	213.96	0.0001	0.928
	3.00	5	0.4486	1367.12	0.0072	0.824	1428.57	1367.12	0.0001	0.998
	3.00	7	0.4219	1049.55	0.0062	0.919	1111.11	1049.55	0.0001	0.999
	3.00	9	0.0418	931.31	0.0057	0.223	909.09	931.31	0.0040	0.999
	3.00	11	0.2543	588.96	0.0088	0.500	588.24	588.96	0.0004	0.988
BCH-C-Tab	3.00	5	0.1103	411.04	0.0012	0.055	416.67	411.04	0.0026	0.999
	3.00	7	0.2227	305.18	0.0068	0.534	312.50	305.18	0.0014	0.996
	3.00	9	0.2594	209.46	0.0041	0.738	208.33	209.46	0.0008	0.998
	3.00	11	0.0249	301.80	0.0041	0.236	303.03	301.80	0.0064	0.999
BCH-Tween 80	3.00	5	0.3233	415.54	0.0056	0.847	416.67	415.54	0.0004	0.999
	3.00	7	0.2472	296.17	0.0058	0.618	303.03	296.17	0.0008	0.999
	3.00	9	0.0500	184.68	0.0011	0.049	181.82	184.68	0.0028	0.999
	3.00	11	0.2119	282.66	0.0021	0.293	277.78	282.66	0.0009	0.995

5.3. Adsorption mechanism

From all of above, the mechanism of adsorption is still not revealed. Therefore, the intraparticle diffusion was employed to describe the adsorption mechanism [43, 50, 51, 57, 58]. The fraction approach to equilibrium change according to a function of $(Dt/r^2)^{1/2}$, where r is the particle radius and D is the diffusivity within the particle. The initial rates of intraparticle diffusion are obtained by linearization of the plot

$$q_t = k_t t^{0.5} \qquad (5.55)$$

where k_i is the intraparticle diffusion rate constant (g/g $min^{-0.5}$). k_i is obtained as the slope of straight-line portions of plot q_t versus $t^{0.5}$. The experimental data may present a multi-state linearity. Each state implies a step of adsorption mechanism. The slope of each stage is termed as the rate parameter $k_{p,i}$(i = 1 – 4). Figure 5.6 and Table 5.7 presents the rate parameter k_{pi} for chitosan and blended chitosan/PVA 1:1. It was found that, (at cutting fluids concentration 0.10 - 3.00 % w/v and pH 3 – 11), the first state for these adsorbents is higher than the second stage because this is the instantaneous adsorption stage. The second stage is an equilibrium stage where the intraparticle starts to slow down due to extremely low cutting fluids concentration in the emulsion.

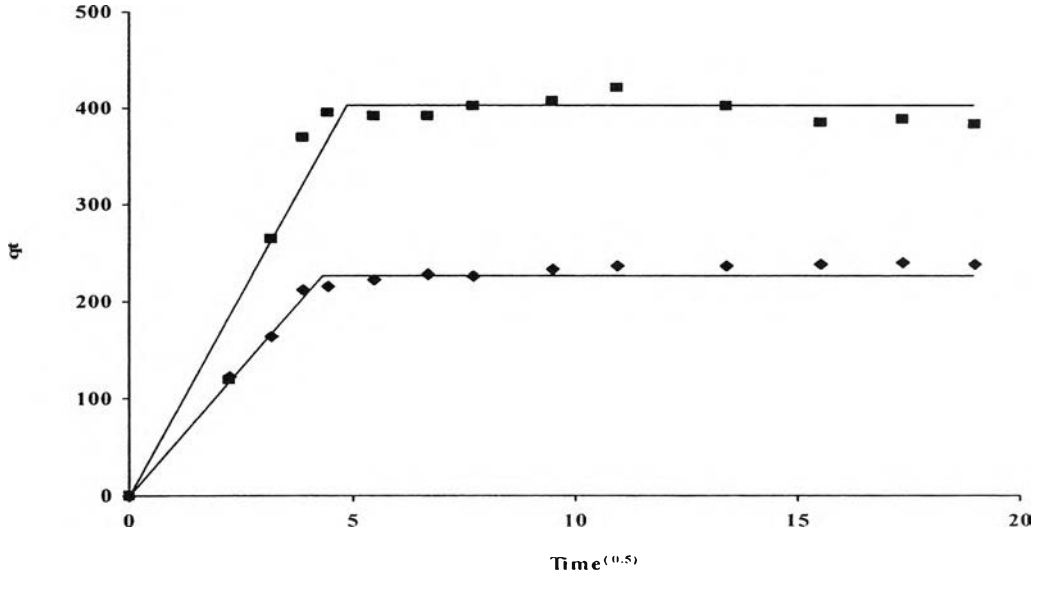

Figure 5.6 Intraparticle diffusion kinetics of cutting fluids by ♦ chitosan and ■ blended chitosan/PVA 1:1

Table 5.7 Rate parameter of intraparticle diffusion for cutting fluids adsorption on chitosan and blended chitosan/PVA 1:1

Adsorbents	Concentration (w/v)	pH	Rate parameter, k_{pi} (i= 1-4) (mg/g $min^{-1/2}$)			
			k_{p1}	k_{p2}	k_{p3}	k_{p4}
Chitosan	0.10	3	1.224	0.084	-	-
	0.50	3	3.349	0.297	-	-
	1.00	3	13.639	1.245	-	-
	3.00	3	7.343	0.360	-	-
	1.00	5	2.994	1.245	-	-
	1.00	7	3.315	0.126	-	-
	1.00	9	3.097	0.439	-	-
	1.00	11	3.174	0.051	-	-
Blended chitosan/PVA 1:1	0.10	3	1.733	0.192	-	-
	0.50	3	0.753	0.034	-	-
	1.00	3	17.329	0.472	-	-
	3.00	3	12.871	0.155	-	-
	1.00	5	3.235	0.598	-	-
	1.00	7	2.238	0.063	-	-
	1.00	9	3.309	0.182	-	-
	1.00	11	3.597	0.155	-	-

Table 5.8 shows the rate parameters of benzoyl chitosan and quateraminated chitosan as adsorbents. It is clearly seen that the adsorption on both adsorbents suddenly occurs in the first stage, when comparing with the second stage. The third and fourth stages of both adsorbents did not appear. This implies that the first stage is the instantaneous adsorption stage of both adsorbents. The second stage is intraparticle diffusion control.

Table 5.8 Rate parameters of intraparticle diffusion for cutting fluids adsorption on benzoyl chitosan and quateraminated chitosan

Adsorbents	Concentration (w/v)	pH	Rate parameter, k_{pi} (i = 1-4) (mg/g $min^{-1/2}$)			
			k_{p1}	k_{p2}	k_{p3}	k_{p4}
Benzoyl chitosan	0.20	3	2.104	0.627	-	-
	1.00	3	9.408	0.118	-	-
	2.00	3	8.499	1.888	-	-
	3.00	3	6.277	1.325	-	-
	1.00	5	4.480	0.345	-	-
	1.00	7	4.289	0.635	-	-
	1.00	9	2.743	0.863	-	-
	1.00	11	3.371	0.943	-	-
Quateraminated chitosan	0.20	3	2.067	0.084	-	-
	1.00	3	10.657	0.532	-	-
	2.00	3	14.347	4.957	-	-
	3.00	3	4.635	2.308	-	-
	1.00	5	4.218	0.064	-	-
	1.00	7	5.694	0.722	-	-
	1.00	9	5.552	1.809	-	-
	1.00	11	3.784	0.187	-	-

Table 5.9 shows the rate parameters of CH-SDS, CH-C-Tab and CH-Tween 80 as adsorbents. It was noticed that the rate parameters is changed when changing in cutting fluids concentration.

In case of CH-C-Tab and CH-Tween 80 shows that the adsorption on CH-C-Tab and CH-Tween 80, the adsorption suddenly occurs in the first stage when comparing with the second stage. The third and fourth stages of CH-C-Tab and CH-Tween 80 adsorbents did not appear. It is suggested that the first stage is the instantaneous adsorption stage. The second stage is intraparticle diffusion control.

In case of CH-SDS see Table 5.9, the first stage of CH-SDS was the highest of cutting fluids concentration of 2.00 and 3.00 % w/v. The second and the third stages did not appear significant for cutting fluids concentration 2.00 % w/v. The fourth stage

was the intraparticle diffusion of both cutting fluids concentrations. With cutting fluids concentration 2.00 – 3.00 % w/v, the adsorption of CH-SDS occurred instantaneously in the first stage. The second to the third stages were gradual adsorption, where the intraparticle diffusion was the fourth as controlled and equilibrium stage of CH-SDS.

Table 5.9 Rate parameter of intraparticle diffusion for cutting fluids adsorption on CH-SDS, CH-C-Tab and CH-Tween 80

Adsorbents	Concentration (w/v)	pH	Rate parameter, k_{pi} (i = 1-4) (mg/g $min^{-1/2}$)			
			k_{p1}	k_{p2}	k_{p3}	k_{p4}
CH-SDS	0.10	3	0.051	-	-	-
	0.50	3	34.46	3.34	-	-
	1.00	3	110.62	71.78	2.14	-
	2.00	3	184.40	115.41	111.28	19.30
	3.00	3	291.05	113.67	49.90	1.17
	5.00	3	118.67	-	-	-
	10.00	3	58.76	28.92	30.83	56.29
	3.00	5	164.07	41.14	21.18	1.17
	3.00	7	208.38	13.27	7.72	-
	3.00	9	119.93	-	-	-
	3.00	11	104.69	-	-	-
CH-C-Tab	0.10	3	2.55	1.24	-	-
	0.50	3	-	-	-	-
	1.00	3	108.85	3.29	-	-
	2.00	3	625.40	27.42	-	-
	3.00	3	721.51	10.50	-	-
	3.00	5	10.88	0.52	-	-
	3.00	7	19.34	2.62	-	-
	3.00	9	9.96	0.41	-	-
	3.00	11	28.49	0.47	-	-
CH-Tween 80	0.10	3	14.20	-	-	-
	0.50	3	31.94	0.68	-	-
	1.00	3	148.24	4.13	-	-
	2.00	3	399.74	18.47	-	-
	3.00	3	576.81	8.99	-	-
	3.00	5	19.45	4.71	-	-
	3.00	7	53.50	2.43	-	-
	3.00	9	63.85	3.31	-	-
	3.00	11	71.44	0.38	-	-

In case of BCH-C-Tab and BCH-Tween 80 (see Table 5.10) the first stage is the instantaneous adsorption stage of BCH-C-Tab and BCH-Tween 80 adsorbents. The second stage is intraparticle diffusion control.

In case BCH-SDS (see Table 5.10), the first stage is the adsorption stage. The second and the third stage are gradual adsorption. The fourth stage is the intraparticle diffusion.

Table 5.10 Rate parameter of intraparticle diffusion for cutting fluids adsorption on BCH-SDS, BCH-C-Tab and BCH-Tween 80

Adsorbents	Concentration (w/v)	pH	Rate parameter, k_{pi} (i = 1-4) (mg/g $min^{-1/2}$)			
			k_{p1}	k_{p2}	k_{p3}	k_{p4}
BCH-SDS	0.10	3	4.65	1.06	-	-
	0.50	3	80.99	1.61	-	-
	1.00	3	140.08	58.02	19.90	-
	2.00	3	219.10	48.36	47.75	43.55
	3.00	3	372.05	74.52	69.82	31.69
	5.00	3	120.92	24.61	23.44	36.36
	10.00	3	23.72	12.71	-	-
	3.00	5	290.89	36.50	31.60	-
	3.00	7	231.14	40.30	1.37	-
	3.00	9	231.38	7.15	-	-
	3.00	11	67.72	10.09	-	-
BCH-C-Tab	3.00	5	137.45	1.16	-	-
	3.00	7	82.12	5.56	-	-
	3.00	9	52.07	4.19	-	-
	3.00	11	89.69	0.38	-	-
BCH-Tween 80	3.00	5	112.29	8.52	-	-
	3.00	7	67.56	2.54	-	-
	3.00	9	61.11	1.04	-	-
	3.00	11	86.77	1.66	-	-

From all of above, it can be supposed to a mechanism adsorption of chitosan, blended chitosan/PVA 1:1, benzoyl chitosan, quateraminated chitosan, CH-C-Tab, CH-Tween 80, BCH-C-Tab and BCH-Tween 80. The emulsion attachs at the outside surface of chitosan, blended chitosan/PVA 1:1, benzoyl chitosan, quateraminated

chitosan, CH-C-Tab, CH-Tween 80, BCH-C-Tab and BCH-Tween 80. It does not move into the internal surface of these adsorbents due to their protonated amino group. The emulsion is clogged up at the surface of these adsorbents. In case of CH-SDS and BCH-SDS, the emulsion moves to the surface of CH-SDS and BCH-SDS. The emulsion may reshape a sphere to an elliptical reduced size. After that, the emulsion moves to small pores and attach tightly to the surface of CH-SDS and BCH-SDS due to their hydrophobic property.

5.4. Effect of temperature on adsorption

In order to study the effects of temperature on adsorption of cutting fluids effluents on chitosan, blended chitosan/PVA 1:1, benzoyl chitosan, quateraminated chitosan, CH-SDS, CH-C-Tab, CH-Tween 80, BCH-SDS, BCH-C-Tab and BCH-Tween 80. The experiments were performed at 33, 38, 43 and 48 ^{0}C. The rate of adsorption can be described as being proportional to the concentration of cutting fluids, if first-order-kinetic is assumed.

$$-\frac{dC}{dt} = K_d C_a \qquad (5.56)$$

where K_d is the adsorption rate constant (min^{-1}), C_a is the concentration of cutting fluids effluent at any particular time (mg/l).

Integrating and rearranging the Equation 5.56 gives

$$\ln\frac{C_t}{C_0} = -K_d t \qquad (5.57)$$

K_d can be calculated from slope of the plot between ln[(C_t/C_0)] and t. The energy and entropy of adsorption can be estimated by the use of absolute reaction states [59]. The adsorption rate constant can be expressed in terms of enthalpy and entropy by the following equation

$$K_d = \left(\frac{\kappa T}{h_p}\right) e^{(\Delta S/R)} e^{(-\Delta H/RT)} \qquad (5.58)$$

where h_p is the Planck's constant (J-sec), R is the gas constant (J/mol-K), T is the absolute temperature (K), ΔH is the enthalpy change during adsorption (kJ/mol), ΔS is the entropy change during adsorption (J/mol-K), κ is the Boltzmann's constant (J/K)

Plot of $\ln(K_d/T)$ versus 1/T gives a value of (ΔH/R) from its slope. Therefore, enthalpy and entropy are obtained. The Gibb free energy of activation may be determined in terms of entropy and enthalpy according to

$$\Delta G = \Delta H - T\Delta S \qquad (5.59)$$

where ΔG was the Gibb free energy (kJ/mol)

Another important thermodynamic parameter is Arrhenius.

Accorrding to Arrhenius law

$$K_d = Ae^{(-E_a/RT)} \qquad (5.60)$$

where A is the Arrhenius energy (min^{-1}) and E_a is the activation energy (kJ/mol)

The values of E_a and A are determined from the slope and intercept of plot $\ln(K_d)$ versus 1/T.

Results of influence of temperature on adsorption of cutting fluids effluents at pH 3 described as following. The equilibrium adsorption capacity increases with temperature, indicating that a high temperature favours cutting fluids effluent removal by adsorption on adsorbents. This effect is a characteristic of a chemical reaction or bond being involved in the adsorption process [59]. By increasing the temperature of adsorption from 33 – 48 ^{0}C, the adsorption capacity of cutting fluids effluent at pH 3 increased from 27.78 – 33.03 mg/g for chitosan, 24.96 – 32.28 mg/g for blended chitosan/PVA 1:1, 20.83 – 32.47 mg/g for benzoyl chitosan, 15.77 – 29.28 mg/g for

quateraminated chitosan, 18.02 – 31.91 mg/g for CH-SDS, 24.59 – 30.78 mg/g for BCH-SDS, 16.89 – 32.85 mg/g for CH-C-Tab, 19.33 – 30.41 mg/g for BCH-C-Tab, 20.27 – 29.84 mg/g for CH-Tween 80 and 18.21 – 25.34 mg/g for BCH-Tween 80.

Increasing in temperature increases the equilibrium conversion. This may be a result of an increase in the mobility of the cutting fluids effluent molecule with temperature. An increasing number of molecules may also acquire sufficient energy to undergo an interaction with active sites at the surface [53]. Furthermore, increasing temperature may produce a swelling effect within the internal structure of the adsorbents enabling cutting fluids effluent to penetrate further. The increase in adsorption is due to changes in pore size, an increase in kinetic energy of the cutting fluids effluent molecules and the enhanced rate of intraparticle diffusion of adsorbate [59]

Results of influence of temperature on adsorption of cutting fluids effluent at pH normal (6.8), is described below. Trending of adsorption capacity of cutting fluids effluent at pH 6.8 is the same as at pH 3. By increasing the temperature of adsorption from 33 – 48 ^{0}C, the adsorption capacity of cutting fluids effluent at pH 6.8 increases from 13.70 – 18.39 mg/g for chitosan, 17.64 – 20.83 mg/g for blended chitosan/PVA 1:1, 36.97 – 48.05 mg/g for benzoyl chitosan, 22.33 – 34.16 mg/g for quateraminated chitosan, 25.71 – 29.65 mg/g for CH-SDS, 18.02 – 25.71 mg/g for BCH-SDS, 19.33 – 22.90 mg/g for CH-C-Tab, 15.02 – 21.58 mg/g for BCH-C-Tab, 13.51 – 21.02 mg/g for CH-Tween 80 and 16.52 – 21.40 mg/g for BCH-Tween 80.

The enthalpy (ΔH) and entropy (ΔS) are determined from the slope and intercept of plot $\ln(K_d/T)$ versus $1/T$. The enthalpy and entropy changes of all adsorbents at pH 3 are summarized in Table 5.11. It was noticed that the enthalpy is positive. This means that the adsorption of cutting fluids effluent at pH 3 is endothermic reaction, so

a increase of temperature encourages cutting fluids effluent adsorption on adsorbents. The enthalpy change of cutting fluids effluent at pH 3 by chitosan, blended chitosan/PVA 1:1, benzoyl chitosan, quateraminated chitosan, CH-SDS, BCH-SDS, CH-C-Tab, BCH-C-Tab, CH-Tween 80 and BCH-Tween 80 as adsorbents was 64.09, 51.75, 54.27, 34.49, 66.94, 63.51, 46.66, 31.80, 14.86 and 18.76 kJ/mol, respectively (see appendix K). The values of enthalpy of adsorption processes may be used to distinguish between chemical and physical adsorption. For chemical adsorption, enthalpy values range from 83 to 830 kJ/mol, while physical adsorption very in range from 8 to 25 kJ/mol [60]. On the basis of the above distinction, cutting fluids effluent adsorption on CH-Tween 80 and BCH-Tween 80 could be a physical adsorption process, while cutting fluids effluent adsorption on chitosan, blended chitosan/PVA 1:1, benzoyl chitosan, quateraminated chitosan, CH-SDS, BCH-SDS, CH-C-Tab and BCH-C-Tab could be a chemical adsorption process. The entropy change is in negative value. This indicates that the adsorption reaction of cutting fluids effluent at pH 3 is not spontaneous. The system gain energy from an external source. This energy is probably obtained through an increase in temperature. The entropy change of cutting fluids effluent at pH 3 by chitosan, blended chitosan/PVA 1:1, benzoyl chitosan, quateraminated chitosan, CH-SDS, BCH-SDS, CH-C-Tab, BCH-C-Tab, CH-Tween 80 and BCH-Tween 80 as adsorbents was -58.56, -100.23, -107.32, -176.15, -54.45, -65.77, -118.54, -168.82, -173.74, and -184.13 J/mol-K, respectively. The entropy change of blended chitosan/PVA 1:1, benzoyl chitosan. quateraminated, CH-C-Tab, CH-Tween 80, BCH-C-Tab and BCH-Tween 80 vary in rang -100 to -185 J/mol-K which may be suggested that these adsorbents presents little adsorption of cutting fluids effluent. On the other hand, chitosan, CH-SDS and BCH-SDS shows

entropy change increasing and vary in range -55 to -66 J/mol-K. It indicated that chitosan, CH-SDS and BCH-SDS presents favorable adsorption cutting fluids effluent.

Arrhenius value is obtained from a series of rate constants measured at different temperatures (ln K_d versus 1/T). The slope and intercept of Arrhenius plot mean an activation energies of adsorption cutting fluids effluents and Arrhenius's energyat pH 3, respectively. The activation energy is summarized in Table 5.11. The activation energy of adsorption cutting fluids effluents at pH 3 are 66.69, 54.36, 56.88, 35.09, 69.55, 21.01, 49.27, 34.40, 17.46 and 21.37 kJ/mol for chitosan, blended chitosan/PVA 1:1, benzoyl chitosan, quateraminated chitosan, CH-SDS, BCH-SDS, CH-C-Tab, BCH-C-Tab, CH-Tween 80 and BCH-Tween 80, respectively. Value of activation energy supports that the rate of adsorption is temperature dependent. In the adsorption process when the rate is controlled by a intraparticle diffusion mechanism, the activation energy is very low and hence it can be concluded that process is controlled by intraparticle diffusion which is a physical step in the adsorption process [53].

The Gibbs free energy of adsorption is calculated from Equation 5.59. It is found that Gibbs free energy of chitosan, blended chitosan/PVA 1:1, benzoyl chitosan, quateraminated chitosan, CH-SDS, BCH-SDS, CH-C-Tab, BCH-C-Tab, CH-Tween 80 and BCH-Tween 80 is positive values. The Gibbs free energies of cutting fluids effluent at pH 3 are 82.44, 83.18, 87.92, 87.71, 84.00, 75.92, 83.83, 84.72, 69.32 and 76.49 kJ/mol for chitosan, blended chitosan/PVA 1:1, benzoyl chitosan, quateraminated chitosan, CH-SDS, BCH-SDS, CH-C-Tab, BCH-C-Tab, CH-Tween 80 and BCH-Tween 80, respectively. This indicates that the adsorption of cutting fluids effluent at pH 3 was not spontaneous. The system gains energy from an external source. This energy is probably obtained through an increase in temperature.

The thermodynamic parameters of pH 6.8 are presented in Table 5.12. It was noticed that the enthalpy is positive. The entropy change is negative and Gibbs free energy is positives values.

Table 5.11 Thermodynamic parameter of cutting fluids effluent at pH 3 of adsorbents

Adsorbents	ΔH (kJ/mol)	ΔS J/(mol-K)	ΔG (kJ/mol)	Ea (kJ/mol)
Chitosan	64.09	-58.56	82.44	66.69
Blended chitosan/PVA 1:1	51.75	-100.23	83.18	54.36
Benzoyl chitosan	54.27	-107.32	87.92	56.88
Quateraminated chitosan	32.49	-176.15	87.71	35.09
CH-SDS	66.94	-54.41	84.00	69.55
BCH-SDS	63.51	-65.77	84.18	21.01
CH-C-Tab	46.66	-118.54	83.82	49.27
BCH-C-Tab	31.80	-168.82	84.72	34.40
CH-Tween 80	14.86	-173.74	69.32	17.46
BCH-Tween 80	18.76	-184.13	76.49	21.37

Table 5.12 Thermodynamic parameters of cutting fluids effluent at pH 6.8 of adsorbents

Adsorbents	ΔH (kJ/mol)	ΔS (J/mol-K)	ΔG (kJ/mol)	Ea (kJ/mol)
Chitosan	45.23	-135.42	87.68	47.83
Blended chitosan/PVA 1:1	31.39	-179.69	87.72	33.99
Benzoyl chitosan	23.83	-197.35	85.70	26.60
Quateraminated chitosan	30.21	.180.95	86.94	32.81
CH-SDS	17.10	-174.40	71.79	19.71
BCH-SDS	15.01	-164.99	66.74	17.62
CH-C-Tab	18.92	-176.07	74.11	21.52
BCH-C-Tab	31.82	-177.67	87.52	34.42
CH-Tween 80	32.35	-176.44	87.66	34.95
BCH-Tween 80	30.59	-181.42	87.46	33.19